Journal of Applied Polymer Science

Cross-linked chitosan beads for phosphate removal from aqueous solution

Mohammad H. Mahaninia, Lee D. Wilson
Department of Chemistry, University of Saskatchewan, Saskatoon, Saskatchewan S7N 5C9, Canada
Correspondence to: L. D. Wilson (E-mail: lee.wilson@usask.ca)

ABSTRACT: Chitosan beads were cross-linked with glutaraldehyde (GA) and epichlorohydrin (EP), respectively, at variable composition. The general features of the adsorptive and textural properties of the bead systems were characterized using *p*-nitrophenolate (PNP) at pH 8.5. As well, a systematic adsorption study of phosphate dianion (phosphate (HPO_4^{2-}) species was carried out in aqueous solution at pH 8.5 and 295 K. The Sips isotherm model yielded adsorption parameters for the chitosan bead systems: (i) monolayer adsorption capacity (Q_m) for PNP ranged from 0.30 to 0.52 mmol g^{-1} and (ii) Q_m values for the bead systems with HPO_4^{2-} ranged from 22.4–52.1 mg g^{-1} for these conditions. GA cross-linked beads reveal greater Q_m values for PNP while EP cross-linked beads showed greater Q_m values for HPO_4^{2-}, in accordance with the surface chemistry and the materials design described herein. The EP cross-linked beads show favorable adsorption–desorption properties and represents a promising tunable adsorbent system for the effective removal of phosphate dianion species in aqueous solution. © 2015 Wiley Periodicals, Inc. J. Appl. Polym. Sci. **2016**, *133*, 42949.

KEYWORDS: adsorption; biopolymers and renewable polymers; cross-linking; porous materials; structure–property relations

Received 17 September 2015; accepted 17 September 2015
DOI: 10.1002/app.42949

INTRODUCTION

Phosphate is a key nutrient in many synthetic fertilizers and it represents a globally important contaminant in aquatic environments due to excessive runoff events, as evidenced by elevated phosphate levels in agricultural areas which employ mineral fertilizers.[1,2] The buildup of nitrogen and phosphorous based fertilizers in aquatic environments has been evidenced by the formation of extensive algae blooms and eutrophication of lakes and rivers.[3] Excess dissolved solids originating from phosphate and nitrate minerals in drinking water are known to contribute to potential hazards to human health such as cardiovascular disease, chronic kidney disease, and mortality.[4] Methods for the physicochemical removal of phosphate include ion-exchange,[5] reverse osmosis,[6] electro-dialysis,[7] iron-aided abiotic nitrate reduction,[8] bioremediation,[9] precipitation,[10] and adsorption processes.[11] Adsorption-based processes are advantageous when compared with other techniques in terms of the infrastructure cost, modular design, simplified technological design, and operation.[12] Diverse types of sorbent materials such as clays, zeolites, and activated carbon materials are commonly used industrial adsorbents for the adsorptive uptake of diverse contaminants in wastewater treatment applications.[13,14]

Chitosan is a linear biopolymer composed of glucosamine and N-acetyl glucosamine that may be isolated by thermal–chemical deacetylation of chitin derived from crustaceans.[15] There is continued interest in biopolymers such as chitosan because it is an abundant and renewable material which can be modified to yield a unique adsorbent material with tunable physicochemical properties.[16] Chitosan beads have widespread application as effective bio-sorbents for the removal of dyes,[17] heavy metals,[15] and inorganic ions.[18] The abundant amino and hydroxyl functional groups of chitosan enable modification *via* cross-linking to yield materials with variable morphology such as powders or beads[18] with variable acid stability, mechanical strength, pore size distribution, and hydrophile–lipophile balance (HLB).[19] Cross-linking of chitosan often results in greater adsorption capacity due to modification of surface area and pore structure properties[12,18,19] due to incorporation of new surface functional groups[20] such as quaternary amines and carboxylate groups.[12]

In this article, we report the synthesis and characterization of cross-linked chitosan beads using glutaraldehyde (GA) and epichlorohydrin (EP) at variable composition (*cf.* Figure 1), along with a study of their equilibrium adsorption properties in aqueous solution with two types of anion species (phosphate dianion and 4-nitrophenolate), respectively. Characterization of the bead materials was carried out using thermal gravimetric analysis (TGA), SEM, FT-IR/UV–Vis spectroscopy, and elemental analysis. The general adsorption properties of chitosan beads

Figure 1. Schematic illustration of the preparation of cross-linked chitosan beads. [Color figure can be viewed in the online issue, which is available at wileyonlinelibrary.com.]

were characterized at pH 8.5 and 20°C using a model organic anion (4-nitrophenolate; PNP) as an adsorptive dye probe to characterize the textural (surface area and pore structure) properties of the chitosan beads. The overall goal of this study was to investigate the sorptive uptake properties of synthetic chitosan bead materials with phosphate dianion species at pH 8.5 and 20°C in aqueous solution. The results of this study will contribute to the development of modified biopolymer materials for the controlled uptake or release of waterborne contaminant oxyanions such as phenolate and phosphate anions. There are sparse examples of systematic studies reporting a comparison of bead materials cross-linked with GA and EP for the uptake efficacy toward phosphate dianion species. A recent example of such a study was reported by Filipkowska *et al.*[21] However, it should be noted that the latter differed from the study presented herein because of the restricted pH conditions (pH 3–4), the lack of structural characterization of bead materials, and the use of a single cross-linker composition. By contrast, the study reported herein covers a wider range of materials composition, materials characterization, and pH conditions which are considered more relevant to wastewater treatment and/or alkaline aquatic environments, where the removal of phosphate dianion species is of greater interest in remediation. This study contributes further to a molecular level understanding of the adsorption properties of these materials toward oxyanions (e.g., HPO_4^{2-}). A unique feature of chitosan materials is their potential utility at alkaline pH conditions since the effective removal of anion species is recognized as a challenging problem,[19] in contrast to existing reports described above. The alkaline solution conditions were chosen to illustrate the unique uptake properties and the potential of such systems toward oxoanion species such as phosphate and phenolate at alkaline pH conditions.

MATERIAL AND METHODS

Materials

GA, EP, and low molecular weight chitosan (75–85% deacetylation, and a molecular weight range: 50,000–190,000 kDa) were obtained from Sigma–Aldrich Canada (Oakville, ON). All materials were used as received without further purification unless specified otherwise.

Synthesis of Cross-Linked Chitosan Beads

Figure 1 shows an illustrative diagram for the preparation of chitosan beads. The following synthetic procedure is briefly summarized. Chitosan (5 g) was dissolved in 2.0% glacial acetic acid solution (250 mL). The chitosan solution was dropped into a 0.5*M* NaOH aqueous solution using a burette with adjustable pipette tips of variable size (100–1000 μL) to enable the formation of spherical chitosan beads with a controlled size range. After imbibing the beads for a minimum of 16 h in aqueous NaOH (0.5*M*), the beads were washed with Millipore water to obtain a neutral pH. The wet beads were cross-linked with 2.5 and 5.0 wt % GA (or EP). The cross-linking reaction occurred for 48 h for GA at pH 7 and 6 h for EP at pH 14 with steady agitation. The cross-linked beads were subsequently immersed for 1 day and washed vigorously with 1 L Millipore water (3×) to remove any unreacted cross-linker. The swelling characteristics of the beads in water were determined by weighing hydrated beads before and after drying at 60°C to determine the hydrated and dry weight. The composition and sample ID of the bead systems are summarized in Table I.

Characterization of Materials

Weight loss profiles of the beads at various temperatures were measured using a thermogravimetric analyzer (TGA; Q50 TA Instruments). Samples were heated in open aluminum pans at 30°C and allowed to equilibrate for 5 min prior to heating at 5°C/min up to 500°C. IR spectra were obtained with a Bio-RAD FTS-40 spectrophotometer, where 6 mg of sample was mixed with 60 mg of spectroscopic grade KBr with a mortar and pestle followed by drying at 60°C. The samples were analyzed as powders in reflectance mode where the Diffuse Reflectance Infrared Fourier Transform (DRIFT) spectra were obtained from multiple scans at 295 K. The spectral resolution was 4 cm^{-1} over the 400–4000 cm^{-1} region. DRIFT spectra were corrected relative to

Table I. Bead Materials with Variable Composition and Cross-linker Glutaraldehyde (GA) and Epichlorohydrin (EP)

Bead materials (sample ID)	Chitosan mass (mg)	Cross-linker wt %[a]	Cross-linker/ chitosan ratio (w/w)[b]	Cross-linker/ chitosan mole ratio[b]	Product yield (%)[c]
Noncross-linked	160 ± 0.05	-	-	-	-
EP 2.5	160 ± 0.05	2.5	1.4	1.7	83
GA 2.5	160 ± 0.05	2.5	1.4	1.6	63
EP 5	160 ± 0.05	5.0	2.8	3.4	65
GA 5	160 ± 0.05	5.0	2.8	3.2	40

[a] wt % is based on the cross-linker weight content in solution used for cross-linking.
[b] Given that the chitosan is fully deacylated, and all chitosan monomers are available for cross-linking.
[c] Given that the average molar mass is 120,000 g mol^{-1}, and amount of residual water content is negligible according to the TGA results, as described in detail in Ref. 30.

a background spectrum of KBr. A Varian Cary-100 Scan UV–Vis spectrophotometer was used to measure the absorbance spectra of PNP ($\lambda_{max} = 400$ nm) directly in aqueous solution. Phosphate levels were indirectly estimated from the formation of a *vanado–molybdo–phosphoric acid* complex using a colorimetric method where the absorbance of the *dye* complex ($\lambda_{max} = 400$ nm) was monitored at steady-state conditions.[22]

ADSORPTION STUDIES

Phosphate Dianion Adsorption Isotherms

Fixed amounts (~10 mg) of each adsorbent (i.e., beads or chitosan powder) were mixed with 10 mL of solution containing adsorbate (phosphate dianion; HPO_4^{2-}) in aqueous solution at pH 8.5 in 6 dram vials at variable concentration (30–200 ppm) of adsorbate and equilibrated at room temperature on a horizontal shaker table (SCILOGEX Model: SK-O330-Pro) for 24 h and 250 rpm. The initial concentration (C_o) was determined before and after adsorption (C_e) at 293 K at pH 8.5. The uptake of HPO_4^{2-} was measured in triplicate and the results were expressed as a difference between concentrations of the initial stock (blank) and residual adsorbate solution after the adsorption process, according to eq. (1). The error bars for the corresponding isotherm results denote the standard error determination.

p-Nitrophenolate (PNP) Adsorption Isotherms

Fixed amounts (~10 mg) of the adsorbent (i.e., beads or chitosan powder) were mixed with 10 mL of PNP dissolved in 0.1*M* aqueous sodium carbonate–bicarbonate buffer using six dram vials at variable concentration of PNP (5–10 mM). Samples were equilibrated at 293 K on a horizontal shaker table (SCILOGEX Model: SK-O330-Pro) for 24 h and 250 rpm. The initial concentration (C_o) was determined before and after adsorption (C_e) in triplicate at pH 8.5. The relative uptake of the adsorbate was determined by difference between the initial blank (C_o) and residual PNP concentration (C_e) in solution after the adsorption process using eq. (1). The error bars for the corresponding isotherm results denote the standard error determination.

Isotherm Equations and Models

The adsorption isotherms are expressed as plots of equilibrium uptake of the adsorbate species by the adsorbent phase from aqueous solution expressed per mass of sorbent (Q_e; mmol/g or mg/g) against the residual equilibrium concentration of unbound adsorbate species (C_e; mM or mg/L). Q_e is defined by eq. (1), C_o is the initial adsorbate concentration, V is the volume of solution, and m is the mass of adsorbent material, as described previously.[23]

$$Q_e = \frac{(C_0 - C_e) \times V}{m} \quad (1)$$

An equilibrium uptake study was carried out with each type of bead material and both adsorbate anions (PNP or HPO_4^{2-}), respectively. The various adsorbent/adsorbate systems were modeled using the Sips isotherm model according to eq. (2).[24,25]

$$Q_e = Q_m \frac{(K_s C_e)^{n_s}}{1 + (K_s C_e)^{n_s}} \quad (2)$$

K_s is the adsorption constant, n_s represents the heterogeneity parameter of the sorbent surface, C_e is the residual adsorbate concentration, and Q_m represents the monolayer adsorption capacity of the sorbent (bead). Equation (2) provides a measure of the heterogeneity of the adsorption process according to the value of n_s[23] and this model accounts for Langmuir behavior when $n_s = 1$. Freundlich behavior is observed when n_s deviates from unity since this model accounts for surface heterogeneities with a distribution of adsorption energy values.[26] The Q_m parameter from eq. (2) enables estimation of the adsorbent surface area (SA; m^2 g^{-1}) by eq. (3) including the accessible surface volume (SV; m^3 g^{-1}) of the sorbent according the quantity of dye adsorbed (V_{ads}) by eq. (4).[23]

$$SA = \frac{A_m \times Q_m \times L}{N} \quad (3)$$

$$SV = \frac{Q_m \times L \times V_{PNP}}{N} \quad (4)$$

Q_m is the monolayer coverage of the adsorbent defined by eq. (2), A_m represents the cross-sectional molecular surface area occupied by PNP (A_m for a *planar* orientation is 5.25×10^{-19} m^2 mol^{-1}; whereas, an *end-on* orientation is 2.5×10^{-19} m^2 mol^{-1}), L is Avogadro's number (mol^{-1}), N is the coverage factor which equals unity for PNP at these conditions, and V_{PNP} is the molecular volume of PNP (9.08×10^{-26} m^3).[23]

Regeneration Study

To study the adsorption–desorption profiles of an optimized chitosan bead system, a cycle of equilibrium adsorption–desorption experiments was performed for EP 2.5. Desorption of

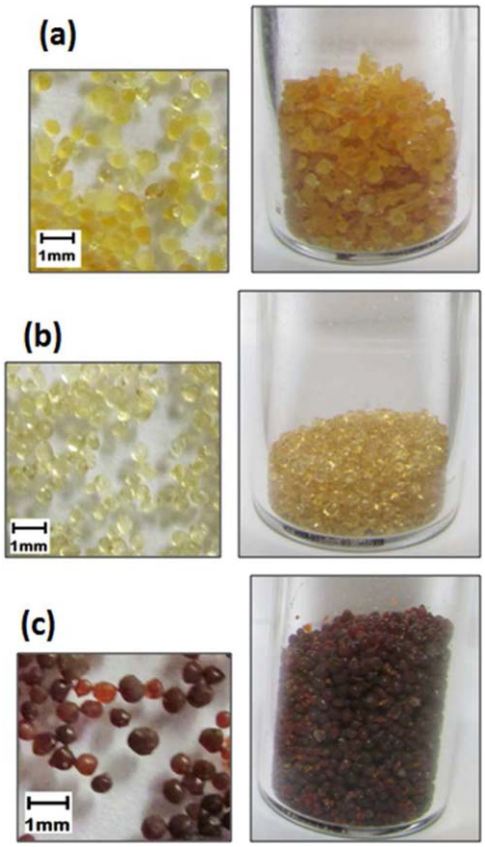

Figure 2. Photograph images of chitosan beads: (a) beads without cross-linking), (b) EP 2.5 beads, and (c) GA 2.5 beads. [Color figure can be viewed in the online issue, which is available at wileyonlinelibrary.com.]

phosphate was achieved by washing the bead adsorbed phosphate using a 50 mM NaCl solution. Since the adsorption of phosphate onto the chitosan beads is assumed to be primarily physical adsorption, saturation of the binding sites with monovalent salt at elevated levels resulted in desorption of the adsorbed phosphate by the chloride anion. The total and residual phosphate concentration was measured in triplicate by UV–Vis spectroscopy, as described for the above isotherm studies above. The error bars for the corresponding isotherm results denote the standard error determination from triplicate uptake measurements.

Diameter and Porosity of Chitosan Beads

Upon imbibing the chitosan beads in a suitable solvent (water), the diameter (D), and the porosity (ε) of wet chitosan beads and swelling properties were determined[27] using eqs. (5–7).

$$D=\left[6\frac{W_D/\rho_{CS}+((W_W-W_D)/\rho_W)}{\pi}\right]^{1/3} \quad (5)$$

$$\varepsilon=\frac{(W_W-W_D)/\rho_W}{W_D/\rho_{CS}+(W_W-W_D)/\rho_W}\times 100\% \quad (6)$$

$$\frac{W_W-W_D}{W_D}\times 100 \quad (7)$$

W_W (g) is the weight of the hydrated bead material after the removal of nonabsorbed water by tamping dry with filter paper; W_D (g) is the weight of the chitosan beads after drying; ρ_w is the density of water (1.0 g cm^{-3}); and ρ_{CS} is the anhydrous density of chitosan (0.87 g cm^{-3}). The density value for the chitosan material in eq. (6) represents the dry weight of chitosan in a hydrated volume of chitosan bead material.

RESULTS AND DISCUSSION

Synthesis of Chitosan Beads

Photograph images of several types of synthetic chitosan bead systems; without cross-linking, including two types of cross-linked beads (EP 2.5 and GA 2.5) are shown in Figure 2. Cross-linked chitosan beads were prepared with variable weight content of GA and EP. The epoxide ring of EP can undergo nucleophilic substitution to form ether bonds *via* the deprotonated hydroxyl groups of chitosan.[28] The aldehyde groups of GA form imine bonds with the amine groups of chitosan at C-2 *via* the Schiff base reaction.[28] The yield was calculated assuming that all the cross-linkers reacted with the monomer units of chitosan according to the mole content of the available amine groups according to the degree of deacetylation. Accordingly, the cross-linking of two chitosan monomers occurs with one equivalent of GA and involves the loss of two water molecules (at pH 5–7), while the cross-linking of two chitosan monomers with EP involves the loss of HCl at alkaline pH.

The diameter (D), porosity (ε), and swelling properties of the different types of hydrated chitosan beads are shown in Table II. A slight reduction in the diameter of the beads was found after cross-linking. This reduction can be related to change in the surface chemistry of the chitosan bead from the addition of the five carbon alkyl group of GA upon cross-linking.[19] The cross-linking of chitosan with EP involves the loss of one OH group for complete reaction of EP. The EP cross-linker unit is estimated to be more hydrophilic in nature relative to GA, as supported by the swelling results of the chitosan bead systems (*cf.* Table II).

Characterization of the Adsorbents

The FTIR spectra of chitosan beads are given in Figure 3(A). The prominent band for each bead material occurs in the 3400–3500 cm^{-1} region corresponding to –OH and $–NH_2$ stretching. IR bands near 2900 cm^{-1} correspond to aliphatic C–H stretching, and the signature at 1635 cm^{-1} corresponds to $–NH_2$, while the band at 1380 cm^{-1} corresponds to –CH symmetric bending vibrations of –CHOH.[12,29] The band near 1100 cm^{-1} was attributed to C–O stretching of C–O–H groups. Since 20–25% of chitosan is acetylated, the corresponding carbonyl signature above 1710 cm^{-1} may be assigned to pendant aldehyde groups where the GA is cross-linked at one end of the linker [*cf.* Figure 3(A); panels c and e]. The vibrational band at 1660 cm^{-1} indicates the carbonyl signature of an acetyl group. The signature at 1640 cm^{-1} overlaps with the imine group and provides support that cross-linking of chitosan occurs with GA.

The level of cross-linking in chitosan beads was estimated by the decomposition profile of the cross-linked beads relative to the thermogram of the unmodified chitosan powder, as shown by the DTG results in Figure. 3(B). A decomposition temperature was observed between 200°C and 250°C for cross-linked beads and at a higher temperature range (250°C and 350°C) for chitosan beads without added cross-linker. The thermal event at 425°C and 475°C correlate to the decomposition of linker units of GA and EP, respectively. The reliability of this approach

Table II. Porosity, Diameter, and Swelling of Different Types of Wet Chitosan Beads

Chitosan beads	Hydrated weight (W_W, g)	Dry weight (W_D, g)	Swelling (%) eq. (7)	Porosity of hydrated beads (ε, %)	Diameter of hydrated beads (D, mm)
Noncross-linked	7.198	0.195	35.91	96.9 ± 0.06	2.40
EP 2.5	6.691	0.182	35.76	96.9 ± 0.06	2.34
GA 2.5	6.912	0.189	35.57	96.9 ± 0.06	2.37
EP 5	6.580	0.179	35.75	96.9 ± 0.06	2.33
GA 5	6.621	0.181	35.58	96.9 ± 0.06	2.33

depends on well resolved thermal stability for chitosan and the respective cross-linker units.

The SEM images of several bead materials are shown in Figure 4. The SEM results illustrate that the cross-linked chitosan beads [*cf.* Figure. 4(c,d)] have a regular microporous structure compared with beads without cross-linking [*cf.* Figure 3(a)]. An image of the hemisphere structure of cross-linked chitosan beads in Figure 4(d,f) reveal that the outer surface layer of beads are amorphous and cross-linked thoroughly, whereas; the core of the bead has a layered textural porosity similar to surface of the bead system without cross-linking.

The calculated surface area (SA) and accessible surface volume (SV) of the various types of chitosan beads are listed in Table V, according to the adsorption parameters derived from the PNP isotherm results. The relative uptake of PNP was reported to be dependent on the surface area, the relative molecular weight, and polydispersity of the chitosan beads.[30] The textural properties and surface chemistry correlate with the cross-linker content, as described elsewhere.[23] According to the results in Table V, a decrease in surface area and accessible surface volume occur as the level of cross-linking increases. Generally, the textural parameters are greater for chitosan cross-linked by GA since pristine chitosan has lower surface area due to its crystalline nature.[19] This trend is compatible with the average size of the pore surface area estimated from the SEM results in Figure 4,[31] and are supported by the results in Table V.

Elemental analyses for the various systems are listed in Table III. While CHN results cannot unequivocally support the type of functional groups, the variable composition of the chitosan beads according to the different types of cross-linkers provides additional support of the cross-linking process. The results from the CHN analysis are unlike the TGA results since a facile qualitative measurement of cross-linker content is possible[19] from the integrated line intensity of the thermogram results (*cf. vide infra*). According to CHN results, the elemental C content (%) would increase as more GA and EP cross-links are formed. As well, there is no N contribution from the EP cross-linker; however, the N content decreases as the level of cross-linking with GA increases. This can be seen where the percent by weight of C increases from 40.9% in noncross-linked chitosan up to 51.4% and 43.3% for GA 2.5 and EP 5 bead systems, respectively. Also, a theoretical calculation for the elemental composition of the beads was carried out to provide further interpretation of the CHN microanalyses results. The theoretical estimates are in reasonable agreement based on residual water content (*ca.* 3–4%) when comparing to the experimental values, where the relative error difference decreases to 3.26%, 0.0%, and 0.96% for CHN contents, respectively.

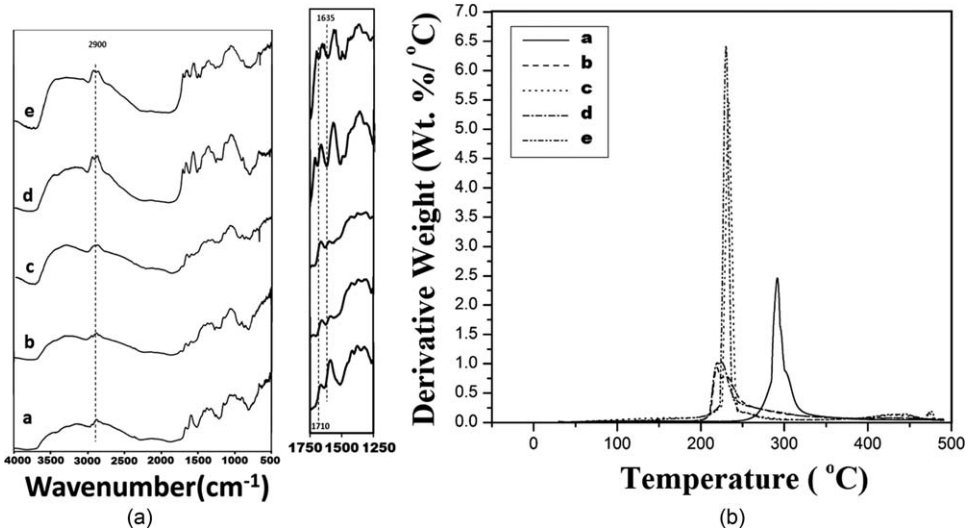

Figure 3. (A) FT-IR spectra and (B) TGA for different chitosan beads; where (a) Chitosan bead without cross-linking, (b) EP 2.5, (c) GA 2.5, (d) EP 5, and (e) GA 5.

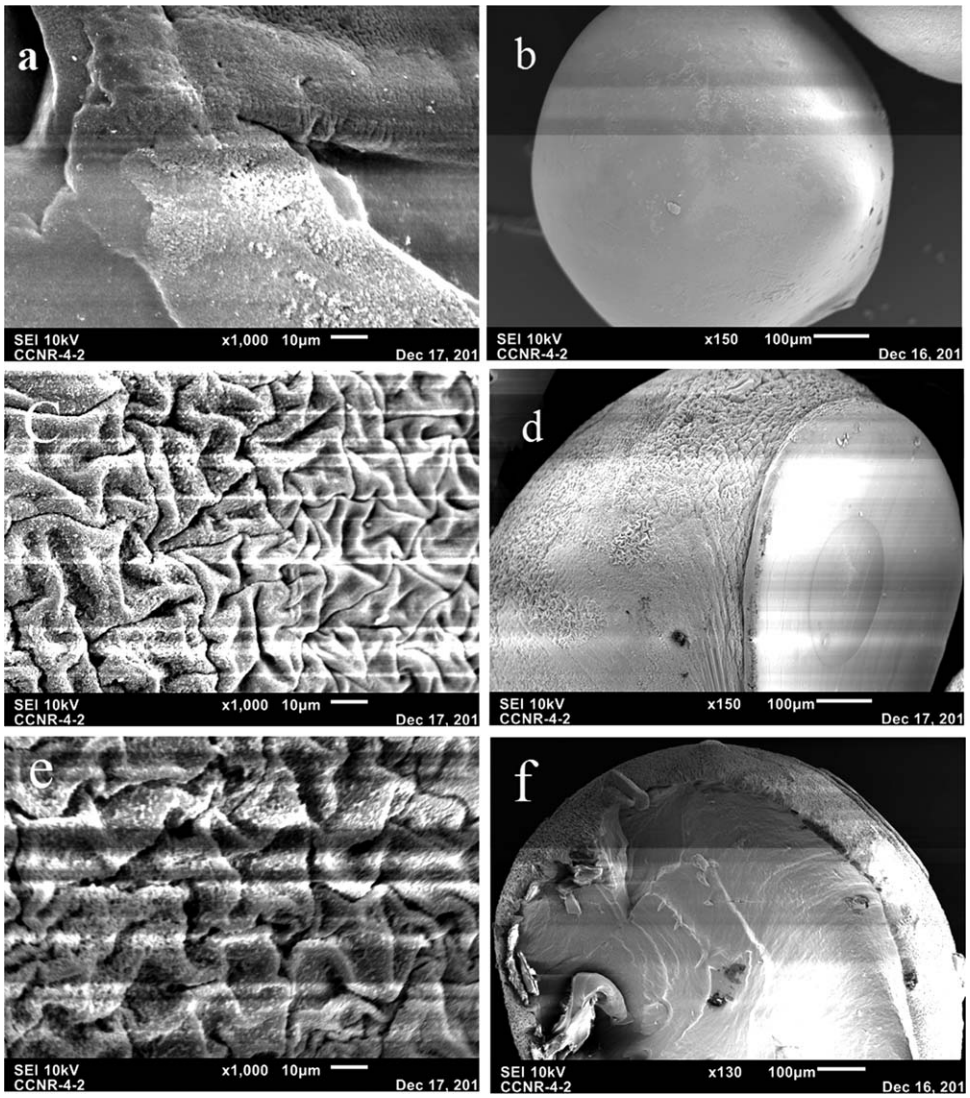

Figure 4. SEM images of (a, b) beads without cross-linking; (c, d) EP cross-linked bead systems; and (e, f) GA cross-linked beads.

ADSORPTION RESULTS

PNP Anion Adsorption Results

The adsorption properties of the chitosan beads were studied in aqueous solution using PNP at pH 8.5 and 20°C. At these conditions, PNP exists as a singly charged anion species since the pH exceeds the pK_a value (7.1) of the PNP dye.[19] PNP is a versatile dye probe for estimating the textural properties of sorbent materials using UV–Vis spectrophotometry.[23] The ionized form of PNP may serve as a surrogate anion suitable for modeling the uptake behavior of inorganic oxyanions,[19] especially singly charged species. The uptake characteristics of the PNP anion can provide insight on the thermodynamics of adsorption processes to afford characterization of the textural (surface area and pore volume) properties[23] of the synthetic chitosan beads. Figure 5 depicts the adsorption isotherm results for PNP at 295 K with different types of bead materials (*cf.* Table I for composition information). The adsorption of noncross-linked beads toward PNP is relatively low and the GA 2.5 bead system has greater uptake toward PNP relative to the other bead materials and is similar to an estimate obtained for cross-linked chitosan powders[30] (*cf.* Table V in Ref. 30) reported at pH 9 in aqueous solution. Interestingly, the value of Q_e for GA 2.5 and EP 2.5 beads exceed those observed for the GA 5 and EP 5 beads. The concentration dependence for Q_e is well-described by the Sips

Table V. Dye-Based Surface Area Estimates of Chitosan Beads with PNP as the Adsorptive Probe in Aqueous Solution at 20°C and pH 8.5

Bead system	SA ($m^2\ g^{-1}$)	V_{ads} ($m^3\ g^{-1}$)	Average pore surface area (m^2)[a]
Noncross-linked	129	24.2	3×10^{-14}
EP 2.5	149	25.7	8.54×10^{-11}
GA 2.5	165	28.5	3×10^{-10}
EP 5	123	21.3	-
GA 5	108	18.6	-

[a] Calculated using SEM images by "ImageJ 1.48" software.

Table III. Elemental Analysis of Chitosan Beads with and without Cross-linking

	Experimental				Theoretical[b]				Differences %			
Sample	C %	H %	N %	O[a]%	C %	H %	N %	O[a]%	C	H	N	O
Noncross-linked	40.9	6.83	7.73	44.5	44.7	6.83	8.69	39.8	3.76	0	0.96	4.75
EP 2.5	41.9	6.71	5.53	45.9	47.1	6.86	7.61	38.4	5.27	0.15	2.08	7.5
GA 2.5	51.4	6.65	4.18	37.8	47.5	6.24	3.21	43.0	3.84	0.41	0.97	5.22
EP 5	43.3	6.48	5.49	44.7	46.6	6.87	7.81	38.8	3.26	0.39	2.32	5.97
GA 5	50.6	6.90	3.93	38.6	46.7	6.51	10.6	36.2	3.92	0.39	6.68	2.37

[a] Calculated by summing the percentages for C, H, and N and subtracting by 100%.
[b] A theoretical calculation for the elemental composition of the copolymers can be calculated by assumptions: known average molar mass (120,000 g mol^{-1}), percentage of deacetylation (80%), residual water of chitosan (negligible according to TGA data), and terminal monomers.

model [eq. (2)], as evidenced by the best-fit line through the experimental data, and the best-fit adsorption parameters listed in Table IV estimated by the Sips isotherm model for the various bead/PNP systems. A comparison of the cross-linked bead systems at variable cross-linker content (wt %) reveals that the Q_m values follow a reverse-ordering according to the relative cross-linker content. As the EP content (wt %) increases, the Q_m values decrease for this bead system. By contrast, the bead systems cross-linked with GA have greater PNP uptake, according to the Q_m values listed in Table IV. A comparison of the noncross-linked chitosan beads and the cross-linked systems reveal that the variable uptake properties are related to structural differences of the cross-linkers (GA vs. EP) and their physicochemical properties. The variation in the uptake of PNP uptake can be related to variable textural and surface chemistry effects, as described in further detail by Wilson *et al.*[23] Surface effects are known to influence the hydration properties of cross-linked chitosan because of the HLB character for each cross-linker system varies according to the composition of the cross-linked bead system, as described above.

Phosphate Dianion (HPO_4^{2-}) Adsorption Results

Figure 6 illustrates the adsorption isotherms of phosphate ion with different chitosan beads in aqueous solution. In general, the adsorption of phosphate dianion for each type of bead increases nonlinearly as C_e increases until the surface sites become saturated at elevated adsorbate levels. By comparison, the adsorption of noncross-linked beads toward phosphate species is relatively low. At these alkaline conditions (pH 8.5 and 20°C), phosphate exists as a dianion (HPO_4^{2-}) species[12] and the isotherm behavior is well described by the Sips model.[23] The adsorption capacity of the beads decrease as the level of cross-linking increases, according to the following: EP 2.5 > GA 2.5 > EP 5 > GA 5. Table IV shows the best-fit parameters for each sorbent material. Overall, the isotherm results for the bead/HPO_4^{2-} systems are well-described by the Sips model, according to the goodness-of-fit results in Table IV. In Figure 5, the Q_e values for various beads show an incremental uptake of phosphate as C_e increases, in agreement with the variable adsorption affinity for each chitosan bead/HPO_4^{2-} system. The value of Q_m for the bead system without cross-linking is lower than the cross-linked beads, in accordance with the nature and composition of the cross-linker employed. The Q_m values for both GA and EP beads adopt a reverse ordering (decreasing uptake) as the cross-linker content increases. This trend may be understood on the basis of the polar nature of the OH group at the C-2 skeletal carbon position on the propyl moiety of EP at the cross-linked bead surface. Greater cross-linking is not anticipated to significantly reduce the available surface adsorption sites but it may contribute to steric effects that hinder diffusion of the phosphate anion into the micropore domains of the chitosan beads. The Sips isotherm provides a good description of the uptake behavior for the various bead systems, as evidenced by the best-fit results. The heterogeneity parameter (n_s) is near unity and approximates a type of Langmuir adsorption behavior anticipated for these systems. Thus, the bead surface is relatively homogeneous in accordance with the monolayer surface coverage anticipated for the adsorption of such divalent phosphate anions.

As indicated above, the adsorption properties of beads cross-linked with EP or GA cross-linkers tend to show variable uptake toward singly charged PNP and phosphate dianion species, respectively. This effect is consistent with the fact that PNP possesses a lipophilic phenyl ring moiety that differs relative to the more hydrophilic phosphate dianion (HPO_4^{2-}). The charge

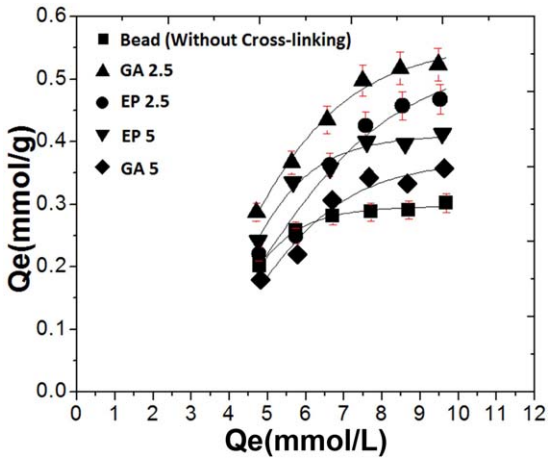

Figure 5. Sorption isotherms for PNP with different various bead materials at 20°C and pH 8.5. The error bars for the corresponding isotherm results denote the standard error determination. [Color figure can be viewed in the online issue, which is available at wileyonlinelibrary.com.]

Table IV. Sips Isotherm Adsorption Parameters for the PNP Monoanion and Phosphate Dianion Species in Aqueous Solution with Different Beads at 20°C and pH 8.5 (Nonbuffered) in Aqueous Solution

	Adsorption parameters for PNP anion species[a]				Adsorption parameters for HPO_4^{2-} species[b]			
Bead system	Q_m (mmol g^{-1})	K_s (L $mmol^{-1}$)	n_s	R^2	Q_m (mg g^{-1})	K_s (L g^{-1})	n_s	R^2
Noncross-linked	0.31	8.7×10^{-2}	0.24	0.98	22.4	0.03	0.92	0.91
EP 2.5	0.54	4.6×10^{-2}	0.95	0.96	52.1	0.05	0.98	0.98
GA 2.5	0.57	4.1×10^{-2}	1.2	0.99	46.1	0.11	0.65	0.97
EP 5	0.42	3.7×10^{-2}	1.1	0.98	41.1	0.05	0.69	0.92
GA 5	0.37	6.3×10^{-2}	1.1	0.97	36.9	0.06	0.63	0.95

[a] PNP ion is in its ionized state as p-nitrophenolate anion since the solution pH exceeds pK_a value for PNP, where pK_a is 7.1.
[b] Counter ion (Na^+) uptake is being neglected. Phosphate ion is in form of dianion in this condition (i.e., HPO_4^{2-}).

delocalization over the phenyl ring of PNP contributes further to its lipophilic character. The greater uptake of PNP with cross-linked beads containing GA present binding sites that are more apolar in nature relative to EP, and contribute to more favorable adsorption.

Regeneration of EP 2.5

The concentration of bound HPO_4^{2-} for the EP 2.5 bead system is shown in Figure 7 for several *adsorption–desorption* cycles. The adsorption of phosphate approaches equilibrium within approximately 1 h, whereas 95% of the bound phosphate species are desorbed within the first 15 min of the washing process. The EP 2.5 beads were regenerated by washing with water and subjected to additional cycles of adsorption–desorption of phosphate. In Figure 7, the process was repeated for four cycles where the uptake capacity of phosphate was relatively constant (12.6 ± 0.1%) illustrating the efficacy of the beads for recycling and re-use as adsorbents for phosphate uptake. The elution process using NaCl (*aq*) with moderate ionic strength is efficient for the removal of adsorbed phosphate for each cycle, and offers a low-cost method for the regeneration of chitosan beads without intermediate drying steps between adsorption-desorption cycles.

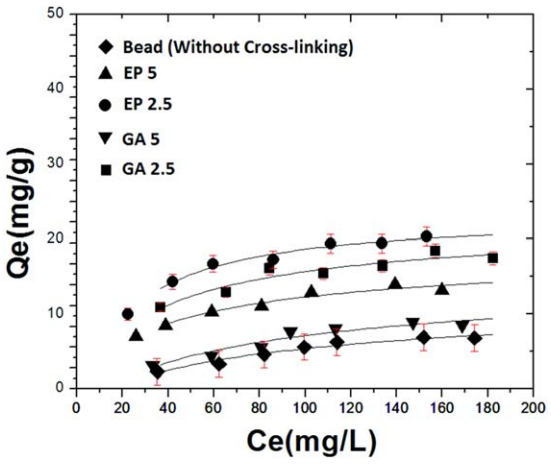

Figure 6. Sorption isotherms of phosphate ion for different bead systems at 20°C and pH 8.5 in aqueous solution. The error bars for the corresponding isotherm results denote the standard error determination. [Color figure can be viewed in the online issue, which is available at wileyonlinelibrary.com.]

Sorbent Surface Area (SA)

The variable sorptive uptake capacity in Table V can be related to the variation in the surface area (SA) of the various bead systems. It is interesting to note that the isotherms for the different bead systems are variable, in accordance with the moderate SA values (107–165 m^2 g^{-1}). GA 2.5 may have greater textural porosity compared with other beads. However, the variable uptake properties are related to two factors; *SA* and type of surface functionalization of the chitosan beads, as supported by the results for bead systems with variable cross-linker (GA and EP) and composition.

Comparison with Other Chitosan Materials

Selected examples of adsorption studies for the uptake of phosphate are listed in Table VI. Sowmya and Meenakshi[12] studied a GA cross-linked chitosan bead at acidic pH conditions for phosphate adsorption with an estimated optimal uptake of 58.5 mg g^{-1}. The study herein has examined the effect of cross-linker type and composition of chitosan bead materials and the adsorption properties with phosphate dianions and PNP species. Poon *et al.*[30,37] reported the preparation of GA cross-linked chitosan in powdered form that involved a systematic adsorption

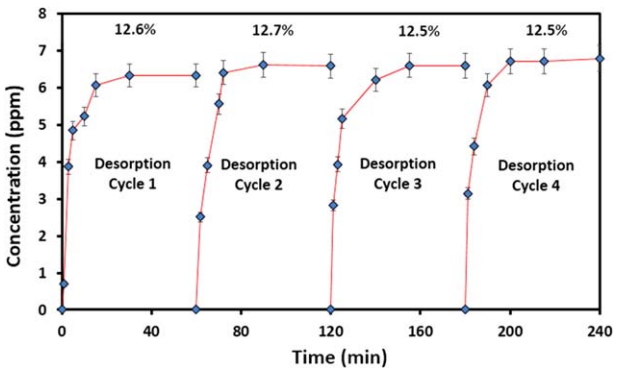

Figure 7. Adsorption–desorption cycle of a phosphate bead (EP2.5)/phosphate dianion system at 293 K. The error bars for the corresponding isotherm results denote the standard error determination. [Color figure can be viewed in the online issue, which is available at wileyonlinelibrary.com.]

Table VI. Chitosan Derivatives Used for the Removal of Phosphate Species and Maximum Adsorption Capacity for Various Chitosan Materials

Adsorbent	pH condition	Adsorption (mg/g)	Reference
Chitosan hydrogel bead/Cu(II) complex	5	88.3[a]	32
Chitosan–melamine–glutaraldehyde resin	3–10	12.5	33
Amine-modified chitosan beads	3–9	59	34
Chitosan-modified zeolite	11	16.2	35
Cross-linked chitosan beads (acidified conditions)	5–7	58.5	12
Carboxylated cross-linked chitosan beads	5–7	48.8	12
Al^{3+}-Cross-linked Chitosan-g-poly(acrylic acid)/vermiculite composite	3–6	22.6	36
Nano-composite Fe_3O_4/ZrO_2/chitosan	3–6	81.1[a]	29

[a] Note: The original reported adsorption capacity was based on phosphorous content.

study of phenolic dyes[30] along with a parallel study of 4-hydroxy-3-nitrobenzene arsonic acid (roxarsone)[37] at variable experimental conditions. The equilibrium uptake results for PNP (*cf.* Table V in Ref. 30 and Table V in Ref. 37) with powdered chitosan polymers reveal that cross-linked chitosan has greater uptake as the cross-linker (GA) content increases. This trend is consonant with the uptake results for chitosan bead materials with PNP and phosphate species reported above (*cf.* Figures 5 and 6). Turning to the results in Figure 6 and Table VI above, EP 2.5 displays favorable adsorption of phosphate dianion ($Q_m = 52.1$ mg g^{-1}) at 295 K and pH 8.5. On the basis of electrostatic effects, the uptake of singly charged phosphate anions ($H_2PO_4^-$) is likely to increase at lower pH (results not shown) for an adsorbent with a neutral surface charge, in agreement with the recent report by Filipkowska *et al.*[21]

Electrostatic interactions and ion exchange are among the various processes that contribute to adsorption of oxyanion species by chitosan.[12,30,37] The mode of interaction between chitosan beads and phosphate dianions are hypothesized to be similar to the mode of interaction for the chitosan/arsenate[38,39] and chitosan/roxarsone[37] systems. Due to the similar structure and protolytic behavior of arsenate and phosphate species, the electrostatic and ion-exchange processes are expected to similarly contribute to the adsorption of HPO_4^{2-} by chitosan materials. In addition, the adsorption of HPO_4^{2-} likely involves hydrogen bonding between the polar functional groups of chitosan (-OH, -NHR; where R = acetyl or H) with the donor–acceptor groups of HPO_4^{2-} to variable extents that depend on the HLB of the bead surface, according to the nature of the cross-linking and composition of the chitosan beads.

CONCLUSION

Cross-linked beads were prepared using a *green* synthetic approach that employs two types of cross-linkers at variable composition (*cf.* Figure 1); EP and GA. The adsorption properties of the bead systems were studied at equilibrium conditions in aqueous solution with PNP and HPO_4^{2-} anion systems. PNP was used as a surrogate dye probe for estimation of the textural properties of the bead systems *via* direct detection with UV–Vis spectrophotometry. PNP was used in an auxiliary dye method to characterize the adsorption properties of various bead systems provided insight on available results of powdered chitosan materials cross-linked with GA.[30,37] Chitosan beads cross-linked with GA had greater uptake of PNP at pH 8.5, while beads cross-linked with EP had greater uptake of HPO_4^{2-} due to differences in the surface chemistry of each bead system. These results are in agreement with the variable hydrophile–lipophile surface characteristics of the chitosan beads, consonant with the type of cross-linker (GA and EP) and relative composition. This study is separate and distinctive from reports[30,37] on chitosan powdered materials due to the unique morphology and surface chemical properties of chitosan bead systems and their wider field of potential applications. The systematic comparison reported herein for the chitosan bead/HPO_4^{2-} systems is highly relevant to remediation of alkaline aquatic environments. The modified biomaterial beads described herein are anticipated to have considerable application in fields of agriculture and environmental science[40] due to their tunable and recyclable properties, especially for the controlled uptake of oxyanion species in aquatic environments. Further studies are underway to evaluate the kinetic uptake properties of phosphate species at various experimental conditions to obtain a more detailed understanding of the adsorption properties of such chitosan bead materials.

ACKNOWLEDGMENTS

The authors are grateful to the Government of Saskatchewan through the generous support of the Agriculture Development Fund (PROJECT#: 20110162). The University of Saskatchewan is acknowledged for supporting this research.

REFERENCES

1. Sattari, S. Z.; Bouwman, A. F.; Giller, K. E.; Van Ittersum, M. K. *PNAS* **2012**, *109*, 6348.
2. Sutton, M. A.; Bleeker, A.; Howard, C. M.; Erisman, J. W.; Abrol, Y. P.; Bekunda, M.; Datta, A.; Davidson, E.; de Vries, W.; Oenema, O.; Zhang, F. S.; including contributions from: Adhya, T. K.; Billen, G.; Bustamante, M.; Chen, D.; Diaz, R.; Galloway, J. N.; Garnier, J.; Greenwood, S.; Grizzetti, B.; Kilaparti, R.; Liu, X. J.; Palm, C.; Plocq Fichelet, V.; Raghuram, N.; Reis., S.; Roy, A.; Sachdev, M.; Sanders, K.;

Scholz, R. W.; Sims, T.; Westhoek, H.; Yan, X. Y.; Zhang, Y. *Our Nutr. World* **2012**, 32.

3. Ozmen, F.; AkkasKavakl, P.; Guven, O. *J Appl. Polym. Sci.* **2011**, *119*, 613.
4. Foley, R. N. *J. Am. Soc. Nephrol.* **2009**, *4*, 1136.
5. Ghafari, S.; Hasan, M.; Aroua, M. K. *Bioresour. Technol.* **2008**, *99*, 3965.
6. Shrimali, M.; Singh, K. P. *Environ. Pollut.* **2001**, *112*, 351.
7. Rautenbach, R.; Kopp, W.; Hellekes, R.; Peter, R.; Vanopbergen, G. *Aqua* **1986**, *5*, 279.
8. Summers, D. P.; Chang, S. *Nature* **1993**, *365*, 630.
9. Akpor, O. B.; Muchie, M. *Sci. Res. Essays.* **2010**, *5*, 3222.
10. Nassef, E. *Estij* **2012**, *2*, 409.
11. Ozturk, N.; Bektas, T. E. *J. Hazard. Mater.* **2004**, *B112*, 155.
12. Sowmya, A.; Meenakshi, S. *Int. J. Biol. Macromol.* **2014**, *64*, 224.
13. Acheampong, M. A.; Meulepas, J. W.; Lens, P. N. L. *J Chem. Technol. Biotechnol.* **2010**, *85*, 590.
14. Kurniawan, T. A.; Chan, G. Y. S.; Lo, W.-h.; Babel, S. *Sci. Total. Environ.* **2006**, *366*, 409.
15. Guibal, E. *Sep. Purif. Technol.* **2004**, *38*, 43.
16. Chatterjee, S.; Chatterjee, B. P.; Guha, A. K. *Colloids Surf. A* **2007**, *299*, 146.
17. Crini, G.; Badot, P.-M. *Prog. Polym. Sci.* **2008**, *33*, 399.
18. Chatterjee, S.; Lee, D. S.; Leec, M. W.; Woo, S. H. *J Hazard. Mater.* **2009**, *166*, 508.
19. Pratt, D. Y.; Wilson, L. D.; Kozinski, J. A. *J. Colloid Interface Sci.* **2013**, *395*, 205.
20. Sun, S.; Wang, L.; Wang, A. *J. Hazard. Mater.* **2006**, *B136*, 930.
21. Filipkowska, U.; Jóźwiak, T.; Szymczyk, P. *PCACD* **2014**, *XIX*, 5.
22. APHA. In Standard Methods for the Examination of Water and Wastewater, 21st ed.; Rice, E. W.; Baird, R. B.; Eaton, A. D.; Clesceri, L. S., Eds.; American Public Health Association: Washington, DC, **2005**; Part 4500P.
23. Wilson, L. D.; Mohamed, M. H.; Headley, J. V. *J. Colloid. Interface Sci.* **2011**, *357*, 215.
24. Sips, R. *J Chem. Phys.* **1984**, *16*, 490.
25. Mohamed, M. H.; Wilson, L. D.; Headley, J. V.; Peru, K. M. *Phys. Chem. Chem. Phys.* **2010**, *13*, 1112.
26. Varum, K. M.; Smidsrod, O. In Polysaccharides—Structure Diversity and Functional Versatility; Dumitriu S., Ed.; Marcel Dekker: New York, **2004**.
27. Zhao, F.; Yu, B.; Yue, Z.; Wang, T.; Wen, X.; Liu, Z.; Zhao, C. *J. Hazard. Mater.* **2007**, *147*, 67.
28. Wan Ngah, W. S.; Endud, C. S.; Mayamar, R. *React. Funct. Polym.* **2002**, *50*, 181.
29. Jiang, H.; Chen, P.; Luo, S.; Tu, X.; Cao, Q.; Shu, M. *Appl. Surf. Sci.* **2013**, *284*, 942.
30. Poon, L.; Wilson, L. D.; Headley, J. V. *Carbohydr. Polym.* **2014**, *109*, 92.
31. Ziela, R.; Hausa, A.; Tulkeb, A. *J. Membr. Sci.* **2008**, *323*, 241.
32. Sowmya, A.; Meenakshi, S. *Desalin. Water Treat.* **2014**, *52*, 13.
33. Dai, J.; Yang, H.; Yan, H.; Shangguan, Y.; Zheng, Q.; Cheng, R. *Chem. Eng. J.* **2011**, *166*, 970.
34. Sowmya, A.; Meenakshi, S. *J. Environ. Chem. Eng.* **2013**, *1*, 906.
35. Xie, J.; Li, C.; Chi, L.; Wu, D. *Fuel* **2013**, *103*, 480.
36. Zheng, Y.; Wang, A. *Adsorpt. Sci. Technol.* **2010**, *28*, 88.
37. Poon, L.; Younus, S.; Wilson, L. D. *J. Colloid Interface Sci.* **2014**, *420*, 136.
38. Sacco, L. D.; Masotti, A. *Mar. Drugs.* **2010**, *8*, 1518.
39. Wilson, L. D. *Water Cond. Purific. Mag.* **2014**, *56*, 28.
40. Udoetok, I. A.; Dimmick, R. M.; Wilson, L. D.; Headley, J. V. *Carbohydr. Polym.* **2016**, *136*, 329.